Influence of operating parameters on morphology of laser hardened surfaces

Maharjan, Niroj; Zhou, Wei; Zhou, Yu; Wu, Naien

2018

Maharjan, N., Zhou, W., Zhou, Y., & Wu, N. (2018). Influence of operating parameters on morphology of laser hardened surfaces. High-Power Laser Materials Processing: Applications, Diagnostics, and Systems VII. doi:10.1117/12.2288890

https://hdl.handle.net/10356/89705

https://doi.org/10.1117/12.2288890

Influence of operating parameters on morphology of laser hardened surfaces

Niroj Maharjan, Wei Zhou, Yu Zhou, Naien Wu

Niroj Maharjan, Wei Zhou, Yu Zhou, Naien Wu, "Influence of operating parameters on morphology of laser hardened surfaces," Proc. SPIE 10525, High-Power Laser Materials Processing: Applications, Diagnostics, and Systems VII, 105250M (15 February 2018); doi: 10.1117/12.2288890

SPIE.

Event: SPIE LASE, 2018, San Francisco, California, United States

Influence of operating parameters on morphology of laser hardened surfaces

Niroj Maharjan[ab], Wei Zhou[a*], Yu Zhou[b], Naien Wu[c]
[a]School of Mechanical and Aerospace Engineering, Nanyang Technological University, 50 Nanyang Avenue, Singapore 639798; [b]Advanced Remanufacturing and Technology Centre, 3 CleanTech Loop, Singapore 637143; [c]Precision Laser Solutions Pte. Ltd, 280 Woodlands Industrial Park E5, Singapore 757322

ABSTRACT

Conventional heat treatment of a component is performed in a furnace whereby the component is continuously heated to a high temperature and quenched to get a hardened material. The furnace heating and tempering process take several hours which is expensive over a long run and less flexible. Laser transformation hardening is an attractive heat treatment technology which can be used to enhance the surface properties of highly stressed components such as cams, gears, and bearings without altering its bulk properties. The highly intense laser beam rapidly heats up the irradiated surface above its austenitization temperature which cools down instantaneously (self-quenching) as the laser moves away from the spot producing a hardened surface. The fast heating and cooling generate a non-equilibrium phase transformation of which very little is understood. An attempt was made to improve the surface properties of steel through solid solution hardening and microstructure refinement using a 250 W fiber laser. To identify the effect of various parameters on laser hardening, scanning conditions such as beam spot size, scan rate, power input, surface condition and overlap ratio were controlled. The change in hardness and morphology of laser treated surface were carefully investigated. The results show the surface hardness increased above 800 HV after laser treatment compared to 260 HV of the as-received specimen. It is found that austenitization has the highest effect on hardness achieved and can be controlled by proper choice of laser parameters and scanning rates.

Keywords: Steel, Heat treatment, Laser hardening, Phase transformation, hardness, austenitization

1. INTRODUCTION

Laser transformation hardening is a surface engineering technique which produces a hard, wear resistant surface using lasers as heat source. The laser delivers sufficient energy to the metal surface in such a way that it quickly increases the surface temperature of the metal above its critical temperature and produces a hard-outer case on rapid cooling[1]. Unlike conventional heat treatment, the process produces minimal distortion, allows treatment of complex shapes and does not require a separate quenching media as the substrate itself acts as heat sink. The method is applied in manufacturing industries to strengthen highly stressed machine parts such as transmission parts, engine components, gears, cams, rock drill parts, shafts and bearings.

Although laser hardening technique has been known to industries for decades, its application was limited primarily due to the high capital cost of the systems. The CO_2 lasers generally used for hardening operations[2–5] were inefficient, bulky and required lots of maintenance cost. With the development of new generation of diode and fiber lasers and advanced optical control systems, the laser systems have become more reliable, efficient and affordable[6]. Now, the major challenge is to understand the interaction of laser with material and how the various operating parameters can be controlled to obtain a desired hardening effect. Previous studies suggest that the laser hardening is affected by various factors such as power density and distribution of laser beam[2], beam spot size and profile[7], laser wavelength used[8], surface absorptivity and surface condition[9] as well as type of material used[10]. The operating parameters are generally correlated to each other and their individual effects are rarely studied. Numerical simulations have been attempted to predict the optimum process conditions and study the properties of hardened surfaces. However, the models are inadequate and can be applicable only for certain conditions.

* wzhou@cantab.net; phone +65 6790 4700

High-Power Laser Materials Processing: Applications, Diagnostics, and Systems VII, edited by Stefan Kaierle, Stefan W. Heinemann, Proc. of SPIE Vol. 10525, 105250M
 · doi: 10.1117/12.2288890

It is thus evident that laser hardening is a complex phenomenon. In this paper, we experimentally explore the individual effects of some of the major operating parameters such as beam spot size, power, speed, surface condition and overlapping ratio on hardening morphology. The resulting morphology and hardness of the surface is also discussed. The results obtained can aid in developing further insights into interaction of laser with steel and can be beneficial for designing of laser hardening system.

2. EXPERIMENTAL METHOD

50CrMo4 steel specimens (AISI 4150) of size 120 mm x 10 mm by 6 mm were used for the study. The nominal composition of the steel is given as follows: 0.48-0.53 C, 0.8 -1.10 Cr, 0.15-0.25 Mo, 0.75-1.00 Mn, 0.15-0.30 Si, 0.035 P max, and 0.040 S max. The specimens were ground progressively using SiC paper up to P2000 grit finish before performing laser treatment.

The laser hardening was performed using an Ytterbium based fiber laser from IPG Photonics (YLR-150/1500-QCW) with wavelength of 1.07 μm. The laser beam was delivered to the work surface by focusing the beam through a lens of 300-mm focal length. The beam had a Gaussian shape distribution. Single line scans of 10 mm were drawn on the sample surface using a galvanometric scanner. All experiments were performed in open air.

In order to study the effect of laser parameters, the power, the speed and the beam spot size of the laser were varied. The laser power and speed used were in the range of 150-250 W and 10-200 mm/s respectively. The beam spot diameter at the specimen surface was varied by moving the sample surface, which is normal to the direction of laser beam, away from the focal plane by a fixed distance. The defocusing distance was varied from 0 to 20 mm at the step of 2 mm. Similarly, two overlapping tracks with different overlap ratios were scanned on the surface to investigate the effect of multitrack laser hardening. A 230 W laser power and 50 mm/s scanning speed was used for defocused and overlapping studies.

Microstructural analyses were carried out using stereomicroscopy, optical microscopy and electron microscopy. The depth and width of laser affected zones was determined from optical micrograph of cross-section after etching with 2% nital solution. Microhardness measurements were made using Vickers' hardness indenter at 100 gf and 15 s dwell time. To reduce error, at least 5 indents were made and average value was taken as the hardness.

3. RESULTS AND DISCUSSION

3.1 Typical microstructures

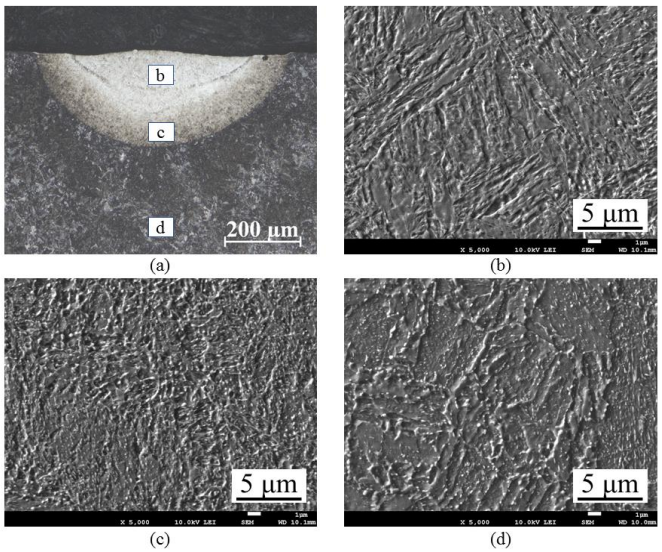

Figure 1. (a) Optical micrograph showing typical microstructures in cross-section of 50CrMo4 steel processed using laser (200 W laser power, scanning speed of 10 mm/s, and spot diameter of 0.5 mm); (b) close-up showing martensitic phase in laser transformed region b; (c) mixed microstructure in region c; and (d) base microstructure.

When a laser beam with sufficient energy is irradiated on a steel surface, the temperature of the irradiated area and the affected zone quickly reaches homogeneous austenitization temperature. This converts the parent ferritic-pearlitic structure to austenite which after the lapse of sufficient time for carbide dissolution, forms martensite structure due to rapid cooling[11]. A typical laser hardened zone with associated microstructure is shown in Figure 1. The laser affected zone can be clearly distinguished from the base microstructure. The structure consists of lath martensite with gradually varying microstructure along the depth. Heat affected zone is minimal or almost absent. At the surface, some oxidation is observed due to reaction of the steel with air as evidenced by presence of oxygen from EDS analysis. Similar microstructures were obtained for all samples.

The size and the properties of the laser transformed zone depends on multitude of factors such as beam spot diameter, energy density input by the laser and the overlap ratio during multi-track scanning. The effects of these individual factors are discussed below.

3.2 Effect of beam spot size

The spot diameter of the laser beam at the specimen surface plays an important role during laser treatment. Thus, the effect of spot size was investigated by defocusing the laser beam. In order to study the depth and extent of hardening, cross section samples normal to laser scan direction were prepared. Figures 2 and 3 show clearly the variation in hardening morphology with change in defocusing distance. The depth of hardening was highest at focused position with value around 120 µm while the width was about 320 µm. The hardening depth decreased with increasing defocusing distance while the width of hardening increased at first and decreased again. The width of hardening remained almost same for 8 mm,10 mm and 12 mm defocused positions and decreased on further defocusing. At 20 mm defocus position, the hardening width reduced to about 250 µm.

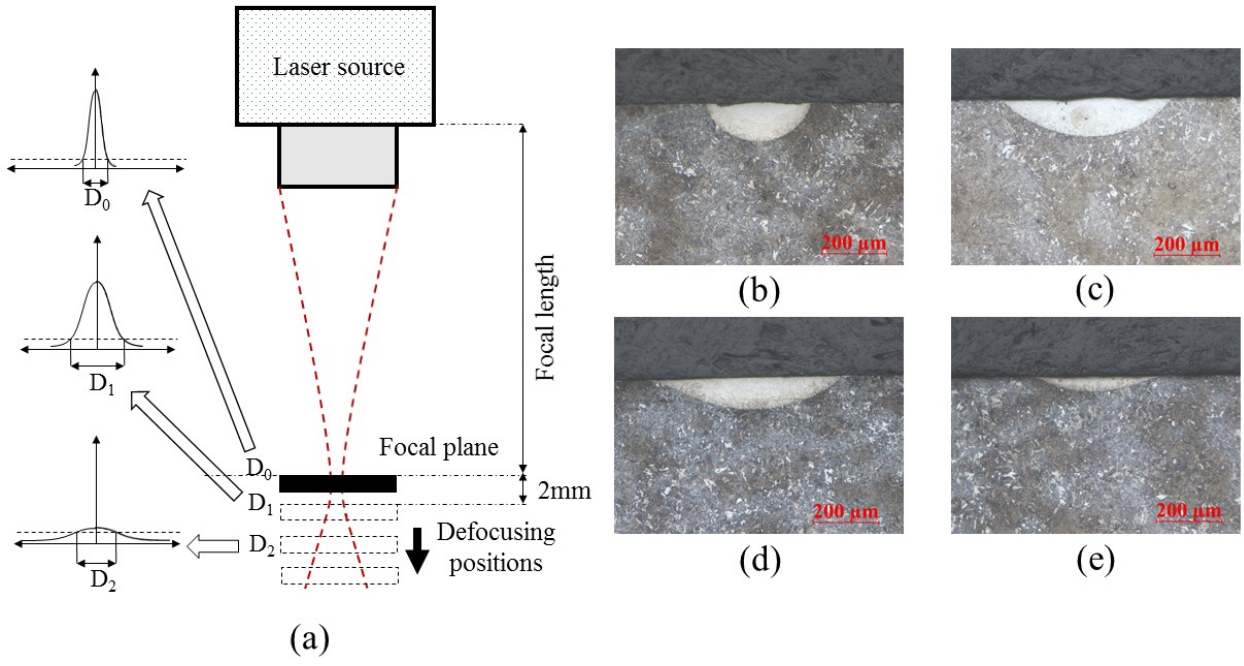

Figure 2. (a) Schematic diagram illustrating defocusing of the laser beam; cross-sections of laser-treated samples at varying defocus distance: (b) 0 mm; (c) 6 mm; (d) 12 mm; and (d) 18 mm.

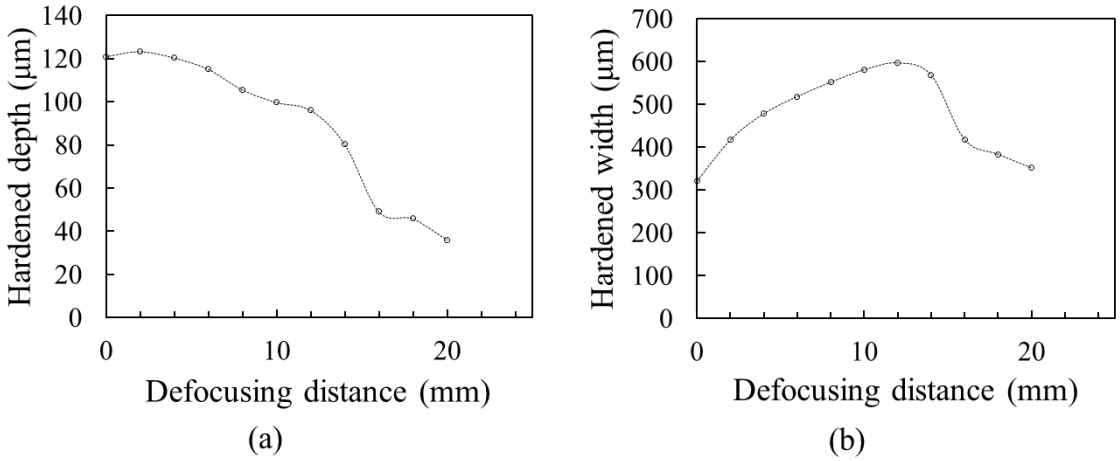

Figure 3. Effect of defocus distance on (a) hardened depth and (b) hardened width.

The variation of microhardness at the surface with change in defocusing distance is shown in Figure 4(a). The difficulty in measuring the indent size gave a wide variation in data for hardness measurement. Nevertheless, the hardness of the laser transformed zone was found to be almost constant and the value was about 800 HV. As mentioned earlier, the variation of width with change in defocusing can be clearly appreciated from the hardness profile as well. It is clear that the width of hardening was minimum at focused condition and increased with increase in defocusing distance before reducing again. Another interesting phenomenon observed was the melting of the surface as shown in Figure 4(b). Surface melting occurred at 0,2,4 and 6 mm defocus positions. On increasing the defocusing distance, it was found that no surface melting occurred from 8 mm onwards. It is also noteworthy to point out the surface distortion was observed due to surface melting in focused condition while no distortion was observed for defocused beam condition.

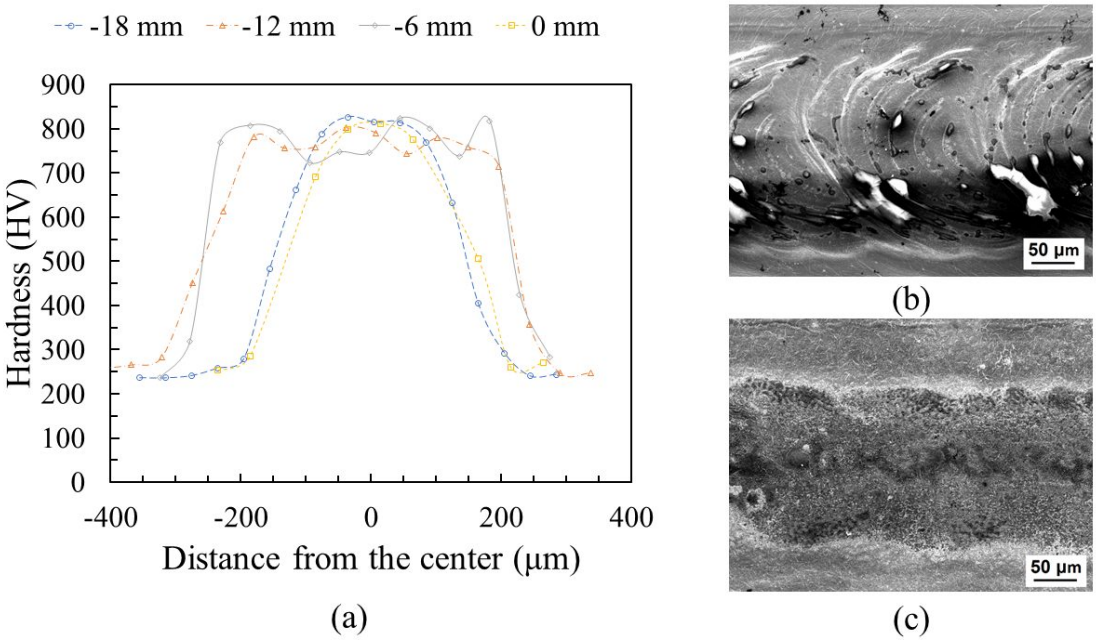

Figure 4. (a) Graph showing variation of surface hardness with distance from the center; (b) surface melting at focused position; and (c) surface at 8 mm defocus position with partial oxidation but no melting.

The results obtained can be explained by the nature of Gaussian beam and the spot size. The Gaussian beam has a normal distribution of energy in a plane perpendicular to the beam axis with maximum at its center as shown in Figure 2(a). Under focused condition, the Gaussian beam has small beam spot size and a high laser energy density. Hence, the high energy density irradiating on a small spot in the surface of the specimen quickly heats up the material beyond its melting point and results in surface melting. Contrary to this, during defocused condition, the beam spot size is large and the energy is normally distributed in the spot area with lower intensity at the edge. Such distribution of laser energy results in a lower peak intensity at the center which is high enough to cause phase transformation, but no surface melting. Consequently, a wider hardening width is generated. On further increasing the defocusing distance, the laser energy density at the edge becomes too low to bring about any phase transformation in the material and hence, it produces a narrower hardening width comparable to the one in focused condition. Based on the result obtained, a 10 mm defocus position was used to produce desired surface hardening effect with minimum surface melting for rest of our experiments. The spot diameter at the specimen surface at this condition is about 500 µm.

3.3 Effect of speed and power variation

The power density of an irradiated area during continuous wave laser treatment can be estimated by $H=P/Dv$, where P is the power input by the laser, D is the laser spot diameter and v is the scanning speed. According to this relation, power density is directly proportional to power supplied by the laser and inversely proportional to the speed and the spot diameter of the laser. In other words, it gives a combined effect of power, speed and beam spot size during laser hardening. To investigate the individual effects of each of these parameters, each factor should be segregated and studied independently.

Figure 5 shows the effect of scanning speed and laser power on depth and width of hardening. Both the hardening width and hardening depth decreased with increase in scanning speed. This is expected since increasing the speed would give less time for laser energy coupling and interaction with the surface resulting in less amount of energy transfer. It is also clear from the graph that both the depth and width increase with increase in laser power used. Thus, a higher extent of hardening is obtained by using a lower scanning speed and a higher laser power.

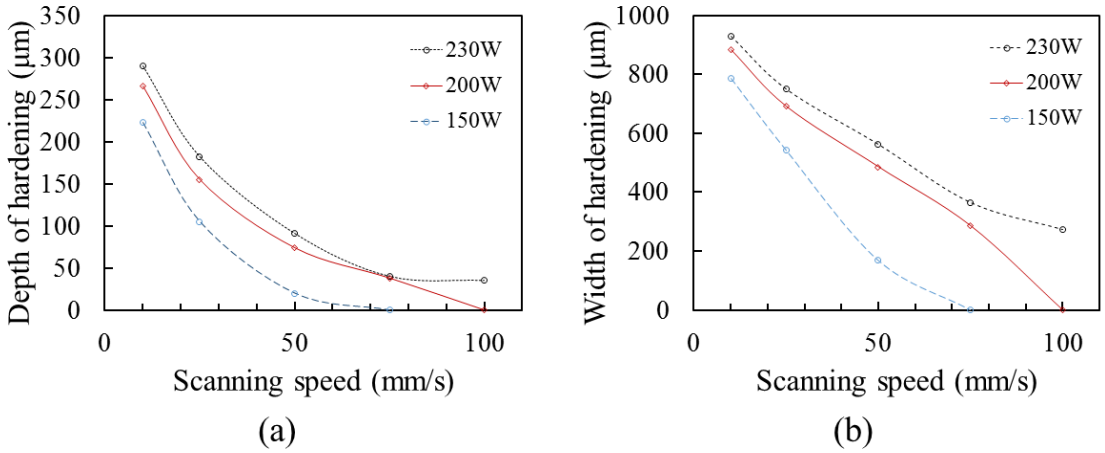

Figure 5. Effect of scanning speed and power on (a) depth and (b) width of hardening.

The hardness of a specimen depends on the distribution of carbide particles in the microstructure and its dissolution during heat treatment. Since the cooling is rapid during laser hardening, austenitization temperature reached plays significant role in resulting microstructure. The material undergoes diffusionless transformation which provides very little time for carbon re-arrangement and forms martensitic structure. A bar chart showing the surface hardness variation with different speed and power is shown in Figure 6. A high hardness is achieved at slower speeds for all power levels used since it reaches higher austenitization temperature and forms smaller martensite sizes (lath and twin) on cooling[4]. The hardness decreased with increase in speed. At faster speed, peak temperature does not exceed the critical temperature required for hardening due to less time for interaction. Thus, it results only in tempering effect which cannot

achieve high hardness value. It is also to be noted that the decrease in hardness is fast for low power than high power. This can be ascribed inadequate heating at low power.

At 10 mm/s speed, it is observed that the highest hardness is obtained for 150 W laser power instead of 250 W power. The time for austenite homogenization can be considered constant for all power levels since same scanning speed is used. However, the higher energy density for 200 W and 230 W power can result in surface melting and decarburization effect which slightly lowers its hardness. For other scanning speeds, this effect is not severe and hence, the general trend of lower hardness with decrease in power prevails.

The hardness of the laser treated area along the depth varies as shown in Figure 7. Initially the hardness is very high near the surface unless there is loss in hardness due to oxidation and surface decarburization which happens usually at high energy density. The hardness decreases gradually along the laser treated area with decrease in extent of laser heating until finally dropping down to base material hardness.

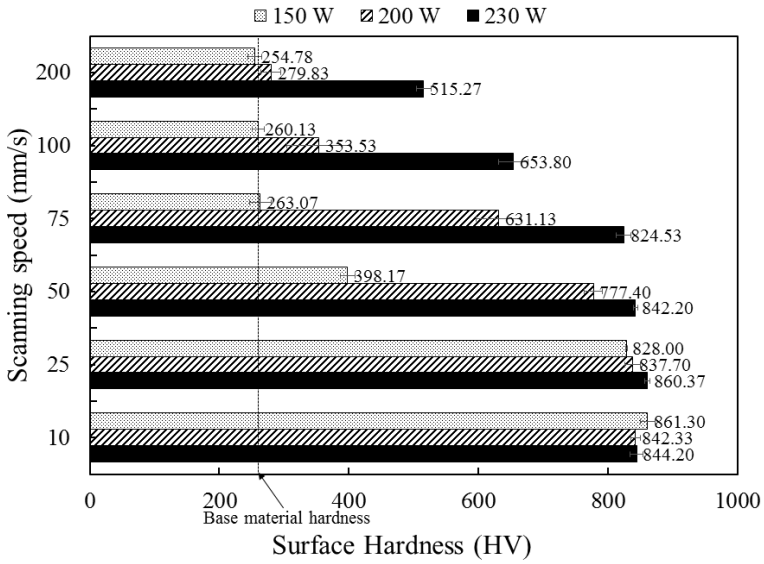

Figure 6. Bar chart showing variation of surface hardness with scanning speed and laser power.

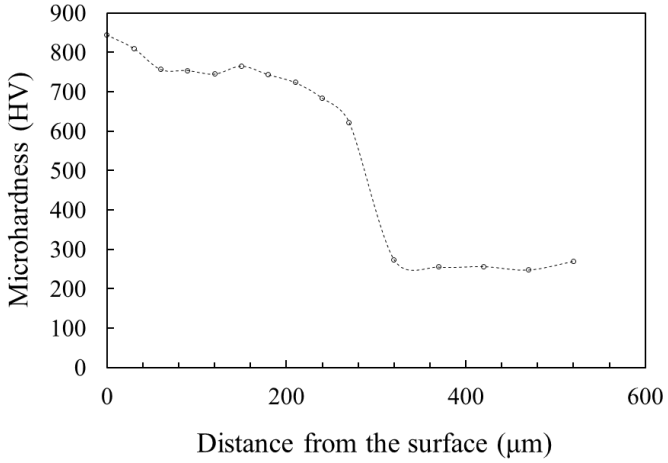

Figure 7. Typical hardness profile along the depth of the sample. (230 W power, 10 mm/s scanning speed).

3.4 Effect of surface oxide layer

In order to study the effect of surface oxide layer, two normalized samples were taken. One of the samples was polished to P1200 grit surface finish while the other sample had an oxide layer fabricated by heating the sample at high temperature in air for several minutes. The surfaces were then laser treated with same laser parameters. The cross section microstructure is shown in Figure 8(a) and (b). It was found that the sample with oxide layer had higher depth compared to polished sample. The oxide layer absorbs more laser energy[12,13] and hence more energy is available for hardening. On the other hand, the width of the laser affected area at the surface for pre-oxidized sample was slightly smaller than that of polished sample. This can arise due to surface decarburization more of which is discussed later.

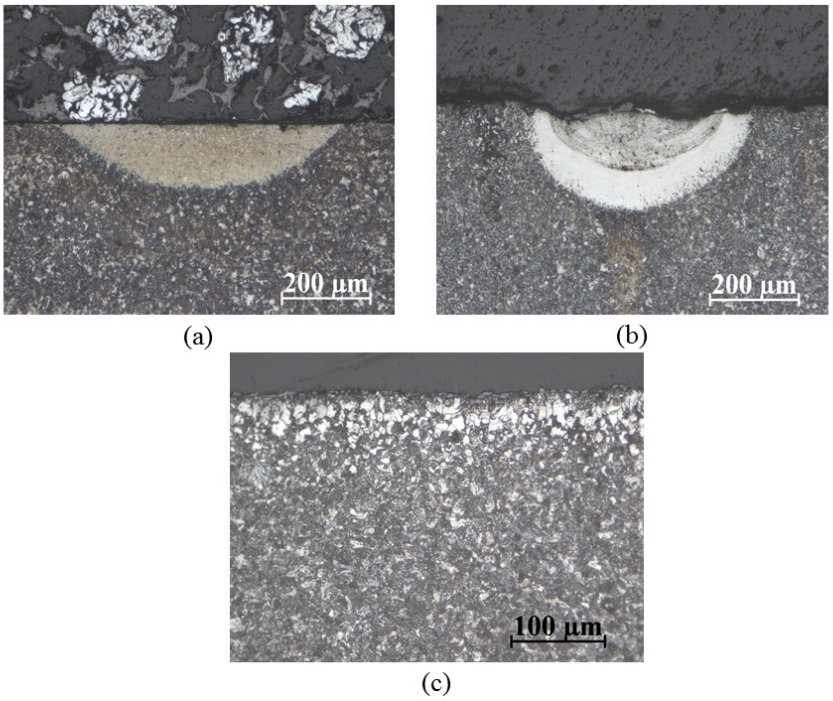

Figure 8. Cross-section of laser hardened region for (a) polished specimen; and (b) pre-oxidized specimen. A smooth hardened surface was obtained in polished sample while the surface melting caused surface distortion in the pre-oxidized sample. Same laser parameters (250W power, 50 mm/s speed and 10 mm defocus position) were used for both experiments. (c) A typical decarburized layer near the surface.

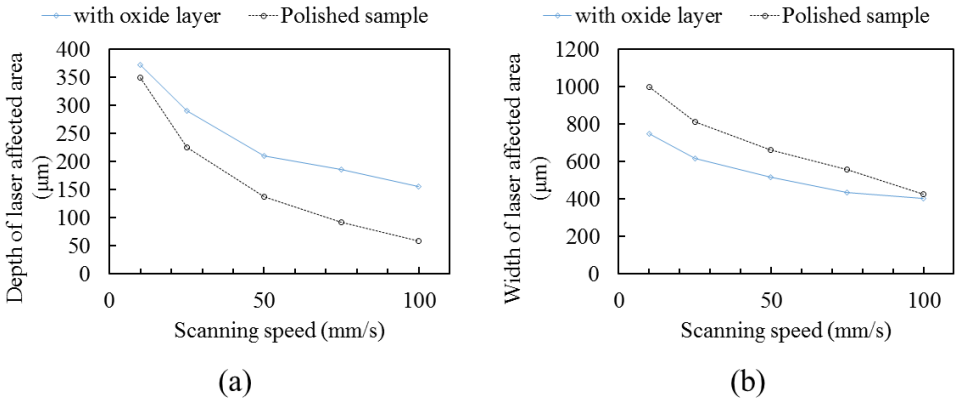

Figure 9. Variation of (a) depth; and (b) width of polished and pre-oxidized specimens with scanning speed.

Figure 10 shows the plot of hardness profile of both samples along the depth direction at the center of laser beam irradiation. For polished sample, the hardness is almost constant at around 800 HV with slight decrease along the depth direction. However, for the pre-oxidized sample, the hardness near the surface was lower (around 600 HV) and gradually increased to about 800 HV before finally dropping to base microstructure hardness. The lower hardness at the surface was attributed to decarburization during pre-oxidation and laser treatment. Decarburization is a well-reported phenomenon understood to occur in oxygen rich atmosphere at temperatures above 700°C[14]. In this process, the carbon diffuses from the metal surface owing to its lower chemical potential in the atmosphere than that in heated steel. The resulting carbon removal from the surface generates the concentration (activity) gradient as driving force of (outward) diffusion which ultimately causes reduction in hardness value near the surface. In addition, the oxide layer on the surface during laser irradiation helps in absorption of laser energy by acting as a blanket to capture the laser light reflected from the metal surface. Thus, abundant heat energy is available at the surface which can result in further oxidation and surface decarburization. The decarburized layer is removed during grinding and polishing and hence no decrease in hardness is observed for the polished sample.

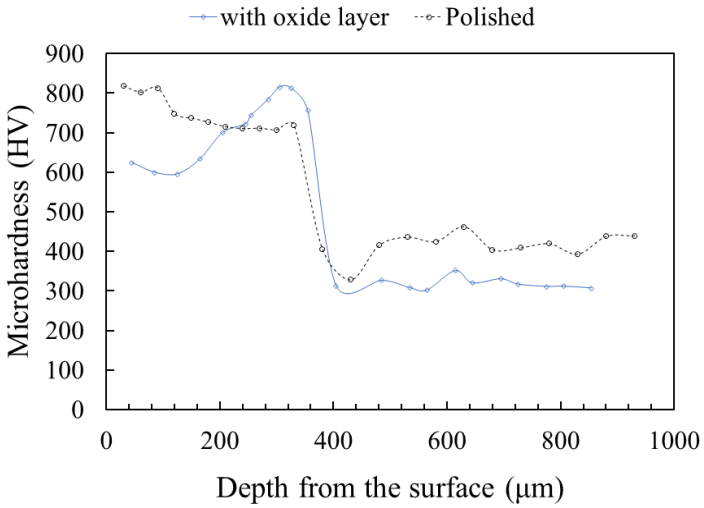

Figure 10. Comparison of hardness profile along depth for different surface conditions.

3.5 Effect of overlapping

In real application, the dimension of the surface to be hardened is generally larger than the spot diameter of laser diameter used for hardening. So, several overlapping tracks are required to harden the whole surface and hence, the distance between the successive tracks significantly affects the hardening obtained. Figure 11 shows the variation of hardness at the surface for different overlapping ratios. The hardness of the first track was lower compared to hardness of the next track. This is due to tempering of the first track due to heating from the successive scan. At higher overlap ratio, the tempering effect was higher which resulted in lower hardness of the first track. While some studies on the effect of overlapping and back-tempering is available[15,16], a detail investigation is yet to carried out.

4. CONCLUSION

This paper investigates the individual effects of operating parameters on laser hardening of steel. Based on the results obtained, the following conclusions are derived:

- Since the cooling is very rapid during laser treatment, the hardness of the steel is primarily determined by the austenitization temperature reached and carbide dissolution in the matrix.

- The beam spot diameter only affects the hardened depth and width. For the range of defocusing distance selected, the surface hardness at the center of the beam spot remains constant irrespective of the spot size since it undergoes same austenitization process for same power and speed.

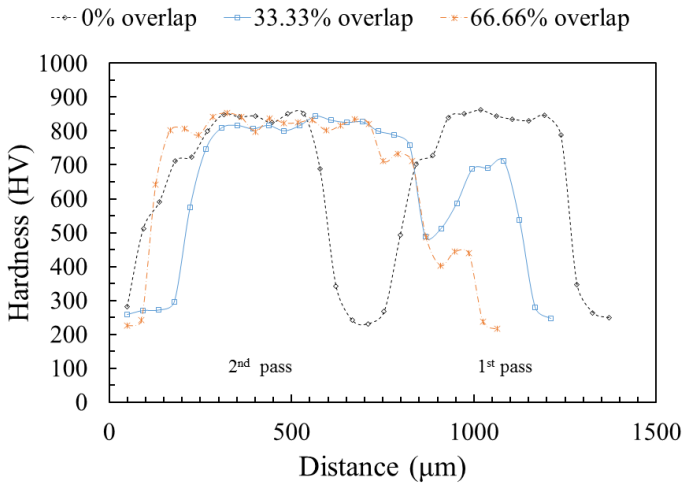

Figure 11.Variation of surface hardness for different overlap ratios

- When the power density is high enough to cause complete austenitization, fast scanning speed produces high hardness value at the surface. The power in such cases has very little effect as long as it is sufficient to ensure heating to austenitization temperature. At high power, however, care must be taken that superheating does not occur which can result in surface melting.
- Presence of oxide layer on the surface increases surface absorptivity. Increased energy absorption contributes to increase in laser affected depth. However, the maximum hardness does not change. Instead, it might result in melting of the surface. Moreover, the hardness at the pre-oxidized surface can decrease due to possibility of decarburization from the surface.
- Overlapping of laser scanning tracks results in backtempering which produces lower hardness. Thus, the optimized scanning track must be used to obtain desired hardening effect on the surface.

ACKNOWLEDGEMENTS

Support from A*STAR SINGA Scholarship, Nanyang Technological University and Advanced Remanufacturing and Technology Center (ARTC), Singapore are gratefully acknowledged.

REFERENCES

[1] Steen, W. M., [Laser Material Processing, Third], Springer (2003).
[2] Steen, W. M. and Courtney, C., “Surface heat treatment of En8 steel using a 2kW continuous-wave CO2 laser,” Met. Technol. **6**(1), 456–462 (1979).
[3] Devgun, M. S. and Molian, P. A., “Experimental study of laser heat-treated bearing steel,” J. Mater. Process. Technol. **23**(1), 41–54 (1990).
[4] Shiue, R. K. and Chen, C., “Laser transformation hardening of tempered 4340 steel,” Metall. Mater. Trans. A **23**(1), 163–170 (1992).
[5] Selvan, J. S., Subramanian, K. and Nath, A. K., “Effect of laser surface hardening on En18 (AISI 5135) steel,” J. Mater. Process. Technol. **91**(1), 29–36 (1999).

[6] Kennedy, E., Byrne, G. and Collins, D. N., "A review of the use of high power diode lasers in surface hardening," J. Mater. Process. Technol. **155–156**(1–3), 1855–1860 (2004).
[7] Sun, P., Li, S., Yu, G., He, X., Zheng, C. and Ning, W., "Laser surface hardening of 42CrMo cast steel for obtaining a wide and uniform hardened layer by shaped beams," Int. J. Adv. Manuf. Technol. **70**(5–8), 787–796 (2014).
[8] Garban-Labaune, C., Fabre, E., Max, C. E., Fabbro, R., Amiranoff, F., Virmont, J., Weinfeld, M. and Michard, A., "Effect of laser wavelength and pulse duration on laser-light absorption and back reflection," Phys. Rev. Lett. **48**(15), 1018 (1982).
[9] Pantsar, H. and Kujanpää, V., "Diode laser beam absorption in laser transformation hardening of low alloy steel," J. Laser Appl. **16**(3), 147–153 (2004).
[10] Bylica, A., Adamiak, S., Bochnowski, W. and Dziedzic, A., "Laser beam hardening of cast carbon steels, plain cast irons, and high-speed steels," Laser Technol. VI, 115–130, International Society for Optics and Photonics (2000).
[11] Krauss, G., "Martensite in steel: strength and structure," Mater. Sci. Eng. A **273**, 40–57 (1999).
[12] Iordanova, I. and Antonov, V., "Surface oxidation of low carbon steel during laser treatment, its dependence on the initial microstructure and influence on the laser energy absorption," Thin Solid Films **516**(21), 7475–7481 (2008).
[13] Cordovilla, F., García-beltrán, Á., Dominguez, J. and Sancho, P., "Applied Surface Science Numerical-experimental analysis of the effect of surface oxidation on the laser transformation hardening of Cr – Mo steels," 1236–1243 (2015).
[14] Alvarenga, H. D., De Putte, T. Van, Van Steenberge, N., Sietsma, J. and Terryn, H., "Influence of Carbide Morphology and Microstructure on the Kinetics of Superficial Decarburization of C-Mn Steels," Metall. Mater. Trans. A **46**(1), 123–133 (2015).
[15] Lakhkar, R. S., Shin, Y. C. and Krane, M. J. M., "Predictive modeling of multi-track laser hardening of AISI 4140 steel," Mater. Sci. Eng. A **480**(1), 209–217 (2008).
[16] Cordovilla, F., García-Beltrán, Á., Sancho, P., Domínguez, J., Ruiz-de-Lara, L. and Ocaña, J. L., "Numerical/experimental analysis of the laser surface hardening with overlapped tracks to design the configuration of the process for Cr-Mo steels," Mater. Des. **102**, 225–237 (2016).